American Heart Association | American Stroke Association®

Impact of Heme and Heme Degradation Products on Vascular Diameter in Mouse Visual Cortex

Alexander Joerk, Raphael Andreas Seidel, Sebastian Gottfried Walter, Anne Wiegand, Marcel Kahnes, PhD; Maurice Klopfleisch; Knut Kirmse, MD; Georg Pohnert, PhD; Matthias Westerhausen, PhD; Otto Wilhelm Witte, MD; Knut Holthoff, PhD

Background—Delayed cerebral vasospasm is the most common cause of mortality and severe neurological impairment in patients who survive subarachnoid hemorrhage. Despite improvements in the field of diagnostic imaging, options for prevention and medical treatment—primarily with the calcium channel antagonist nimodipine or hemodynamic manipulations—are insufficient. Previous studies have suggested that heme and bilirubin oxidation end products, originating from degraded hemoglobin around ruptured blood vessels, are involved in the development of vasospasm by inhibiting large conductance BK_{Ca} potassium channels in vascular smooth muscle cells. In this study, we identify individual heme degradation products regulating arteriolar diameter in dependence of BK_{Ca} channel activity.

Methods and Results—Using differential interference contrast video microscopy in acute brain slices, we determined diameter changes of intracerebral arterioles in mouse visual cortex. In preconstricted vessels, the specific BK_{Ca} channel blockers paxilline and iberiotoxin as well as iron-containing hemin caused vasoconstriction. In addition, the bilirubin oxidation end product *Z*-BOX A showed a stronger vasoconstrictive potency than its regio-isomer *Z*-BOX B. Importantly, *Z*-BOX A had the same vasoconstrictive effect, independent of its origin from oxidative degradation or chemical synthesis. Finally, in slices of Slo1-deficient knockout mice, paxilline and *Z*-BOX A remained ineffective in changing arteriole diameter.

Conclusions—We identified individual components of the oxidative bilirubin degradation that led to vasoconstriction of cerebral arterioles. The vasoconstrictive effect of *Z*-BOX A and *Z*-BOX B was mediated by BK_{Ca} channel activity that might represent a signaling pathway in the occurrence of delayed cerebral vasospasm in subarachnoid hemorrhage patients. (***J Am Heart Assoc***. 2014;3:e001220 doi: 10.1161/JAHA.114.001220)

Key Words: bilirubin oxidation end products • cerebral vasospasm • potassium ion channels • subarachnoid hemorrhage

Subarachnoid hemorrhage (SAH) is a severe acute disease caused primarily by rupture of an intracranial aneurysm with edema and bleeding into the basal cisterns of the brain. Before receiving medical attention, the mortality rate exceeds 12% immediately after this hemorrhagic subtype of stroke.[1] Due to a substantial deterioration of brain function, another 25% of patients die within 24 hours. The remaining survivors often suffered a posthemorrhagic vasospasm of cerebral blood vessels, typically occurring 3 to 9 days after the initial event.[2,3] Symptomatic vasospasm, referred to as "delayed ischemic neurological deficit" (DIND), plays a decisive role of secondary ischemic stroke in more than one-third of post-SAH patients and is characterized by an impaired neurocognitive outcome through long-lasting luminal narrowing of arterial vessels including smaller arterioles. Although the precise pathophysiological mechanism of occlusion remains vague, there is a growing body of evidence that heme and heme degradation products, subsequently liberated from perivascular hematoma, act as major contributors in the development of delayed cerebral vasospasm.[4–8] Besides products of the oxidative degradation of bilirubin and biliverdin detected in cerebrospinal fluid of post-SAH patients who develop vasospasm,[6] the intracranial hemorrhage triggers an inflammatory response including invasion of macrophages and white blood cells that excite expression of heme oxygenase–1 protein.[7,9] This inducible enzymatic isoform metabolizes heme to biliverdin, carbon monoxide, and iron. Biliverdin itself is converted to bilirubin by biliverdin reductase. Previous studies have shown that bilirubin does not cause a vasospastic-like increase of vascular tone.[5] However, free iron released by heme

degradation can react with hydrogen peroxide to form hydroxyl free radicals acting on hemoglobin breakdown products to generate bilirubin oxidation end products (BOXes).[7,8] The equilibrium between vasoconstriction and vasodilation in response to blood pressure and neuronal activity is, under physiological conditions, regulated by large-conductance calcium- and voltage-gated Slo1 potassium channels (BK_{Ca}) located in the plasma membrane of vascular smooth muscle cells (VSMCs). Both the global rise in intracellular calcium concentration ($[Ca^{2+}]_i$), mediated by voltage-dependent calcium channels, and the localized intracellular calcium release, accomplished by inositol trisphosphate receptors and ryanodine receptors in the sarcoplasmatic reticulum membrane, results in BK_{Ca} channel opening.[10] The subsequent potassium efflux leads to membrane hyperpolarization, promoting closure of voltage-dependent calcium channels and thus antagonizing myogenic tone. The sequence analysis of the channel protein identified a long carboxyl extension, assembled with regulatory domains that allow the intracellular sensing across a wide variety of potential ligands including lipids, gaseous molecules, reactive oxygen species, or the inhibitory scorpion venoms iberiotoxin (IbTX) and charybdotoxin.[11] The link between the vasoconstrictive potency of BOXes and the considerable relevance of Slo1 BK_{Ca} channels in the regulation of vascular tone supported the idea that BOXes may influence the gating properties of this potassium channel. Hou et al recently obtained evidence that BOXes decrease the current amplitude and frequency of BK_{Ca} channel opening by binding to the lysine-containing linker segment located downstream of the transmembrane domain.[12] In addition, Tang et al demonstrated that heme (Fe^{2+}) and hemin (Fe^{3+} chloroprotoporphyrin IX) directly reduced the potassium current and decreased the duration of channel opening via heme-binding motif.[13] Apart from large artery vasospasm, the role of brain parenchymal and pial arterioles in the development of DIND is less well investigated. Using in vivo fluorescence microscopy, Friedrich et al have proven that SAH, induced in C57/BL6 mice by endovascular perforation, resulted in microthrombosis and vasoconstriction of pial arterioles.[14]

The aim of our study was to quantify the vasoactive potency of different compounds of heme degradation products on cerebral parenchymal arterioles. Using an in vitro model system, we characterized changes in arteriolar diameter in acute brain slices of wild type and Slo1-deficient ($Slo1^{-/-}$) mice.

Materials and Methods

Chemicals and Reagents

Chemicals were purchased from Sigma-Aldrich (bilirubin, N_ω-nitro-L-arginine methyl ester hydrochloride [L-NAME], IbTX, hemin, paxilline, nimodipine solid), from Frontier Scientific (copper[II] protoporphyrin IX, zinc[II] protoporphyrin IX), from VWR (hydrogen peroxide, high-performance liquid chromatography [HPLC]-grade acetonitrile), from Fisher Scientific (chloroform, ultra-performance liquid chromatography [UPLC]-grade water, UPLC-grade acetonitrile), from Roth (NaCl, magnesium chloride hexahydrate [$MgCl_2$], D-[+]-glucose monohydrate, HCl, formic acid), from Merck ($CaCl_2$, KCl, sodium bicarbonate [$NaHCO_3$], monosodium phosphate [NaH_2PO_4]), from Chempol (sodium hydroxide), and from Biosolve (UPLC-grade formic acid). Water used for HPLC was obtained from a TKA MicroPure system (Thermo Electron).

Liquid Chromatography and Mass Spectrometry

UPLC analysis was carried out using an Acquity UPLC (Waters Corp) equipped with an Acquity UPLC BEH C18 column (1.7 µm, 100×2.1 mm). A multistep gradient (solvent A: 0.1% aqueous formic acid containing 2% acetonitrile; solvent B: acetonitrile containing 0.1% formic acid) was applied with a constant flow rate of 400 µL/min (0 to 0.5 minute: 100% solvent A; 0.50 to 1.50 minutes: 0 to 19% solvent B; 1.50 to 4.25 minutes: 19 to 19.5% solvent B; 4.25 to 6.25 minutes: 19.5 to 100% solvent B; 6.25 to 8.25 minutes: 100% solvent B followed by reequilibration to 100% solvent A). Mass spectra were recorded online on a Waters Micromass Q-ToF Micro mass spectrometer measuring with electrospray ionization in positive-ion mode. Preparative HPLC was performed on a Shimadzu LC-8A using a C18 HTec column (5 µm, 250 × 16 mm; Macherey–Nagel) and an SPD-10AV UV-VIS detector measuring at a wavelength of 310 nm. The HPLC-tandem mass spectrometry method is currently unpublished.

Preparation of Bilirubin Oxidation End Products

With the exception of the synthetic variant of the *Z*-isomer of BOX A (*Z*-BOX A syn), all BOX-containing compounds were prepared by the nonenzymatic oxidative degradation of bilirubin (Figure 3A), modified after Wurster et al.[15] Protected from light, 1 g of bilirubin was dissolved in 500 mL of 5 mol/L sodium hydroxide solution. The mixture was adjusted with 11 mol/L HCl to pH 7.5, and 50% hydrogen peroxide solution was added to a final concentration of 10% by volume. After incubation at room temperature for 48 hours, the yellowish solution was frozen in a bath of liquid nitrogen and freeze-dried to produce the solid crude oxidation product (BOX salt). To prepare BOX extract, the yellowish BOX salt was thoroughly triturated and extracted with 1 L of chloroform. The solvent was removed under reduced pressure. In order to prepare the pure isomers *Z*-BOX A and *Z*-BOX B, the extract was suspended and vortex mixed in acetonitrile/water (20/80 v/v). For purification, aliquots of the supernatant were

separated by preparative reversed-phase HPLC with an isocratic eluent system of acetonitrile/water (20/80 v/v). The manually collected fractions were concentrated to dryness under reduced pressure to obtain the pure solid substances Z-BOX A and Z-BOX B. For short-term storage, all BOX-containing preparations were dissolved in artificial cerebrospinal fluid (aCSF) solution and were aliquoted into sample tubes prior to freezing at −20°C. The selective synthesis of the Z-isomer of BOX A was prepared starting from 3-bromo-4-methylfuran-2,5-dione.[16]

Animals

All animal procedures were approved by the University of Jena and were in accordance with institutional guidelines. Experiments were done on acute brain slices from randomly assigned wild-type C57BL/6J mice at postnatal day 16 to 18 and Slo1 knockout (Slo1$^{-/-}$) mice at postnatal day 16 to 25. Knockout animals were genotyped in the first postnatal week and had a mixed genetic background of FVB and C57BL/6J.

Brain Slice Preparation

After euthanizing under deep isoflurane anesthesia, animals were decapitated. The brain was rapidly removed and transferred into 4°C aCSF containing the following composition (mmol/L): 125 NaCl, 4 KCl, 25 NaHCO$_3$, 1.25 NaH$_2$PO$_4$, 0.5 CaCl$_2$, 6 MgCl$_2$, 10 glucose, bubbled with 5% CO$_2$/95% O$_2$ and adjusted at pH 7.4. Subsequently, 350-μm-thick coronal brain slices, comprising occipital and parietal cortex, were cut using a vibrotome (Leica VT 1200S) and subsequently stored for at least 60 minutes and up to a maximum of 90 minutes at room temperature in aCSF containing 125 NaCl, 4 KCl, 25 NaHCO$_3$, 1.25 NaH$_2$PO$_4$, 2 CaCl$_2$, 1 MgCl$_2$, 10 glucose (in mmol/L), equilibrated with carbogen (5% CO$_2$/95% O$_2$), at pH 7.4. Slices were placed into a recording chamber at the stage of the microscope and continuously perfused with aCSF at 32 to 34°C (flow rate 4 to 5 mL/min).

Optical Imaging

All experiments were performed using near-infrared differential interference contrast video microscopy (Eclipse FN1; Nikon Instruments) in combination with a Rolera XR camera (QImaging) driven by the software StreamPix 5 (NorPix Inc).

Vessel Diameter

Arterioles in layer 2/3 of the primary visual cortex and perpendicular to the cortical surface were selected as structures of interest (Figure 1B). Arterioles differed from venules by their sinuous morphology with visible vascular myocytes and a wall thickness of at least 4 μm. Only vessels with a stable diameter and an intraluminal range of 18 to 30 μm were considered. Medium arteriolar internal diameter was calculated as the area between opposite vessel walls along a length of 50 μm centered around the zone of maximal vascular reaction (Figure 1C). Changes in luminal width were determined by measuring the number of pixels inside this area and were analyzed offline using images acquired at the same field of view every minute. Pixel calibration was carried out by ascertainment of the number of pixels per micrometer. To mimic the myogenic tone, caused by blood pressure in vivo, arterioles were preconstricted by administration of the NO synthase (NOS) inhibitor L-NAME for 20 minutes before administering BK$_{Ca}$ channel inhibitors (Paxilline, IbTX) and before heme and heme degradation products began. To prepare nimodipine solution, the nimodipine salt was dispersed and vortex mixed in aCSF containing 100 μmol/L L-NAME at pH 7.4. Separately for each brain slice, vasoactive substances were dissolved acutely in the prewarmed aCSF control solution.
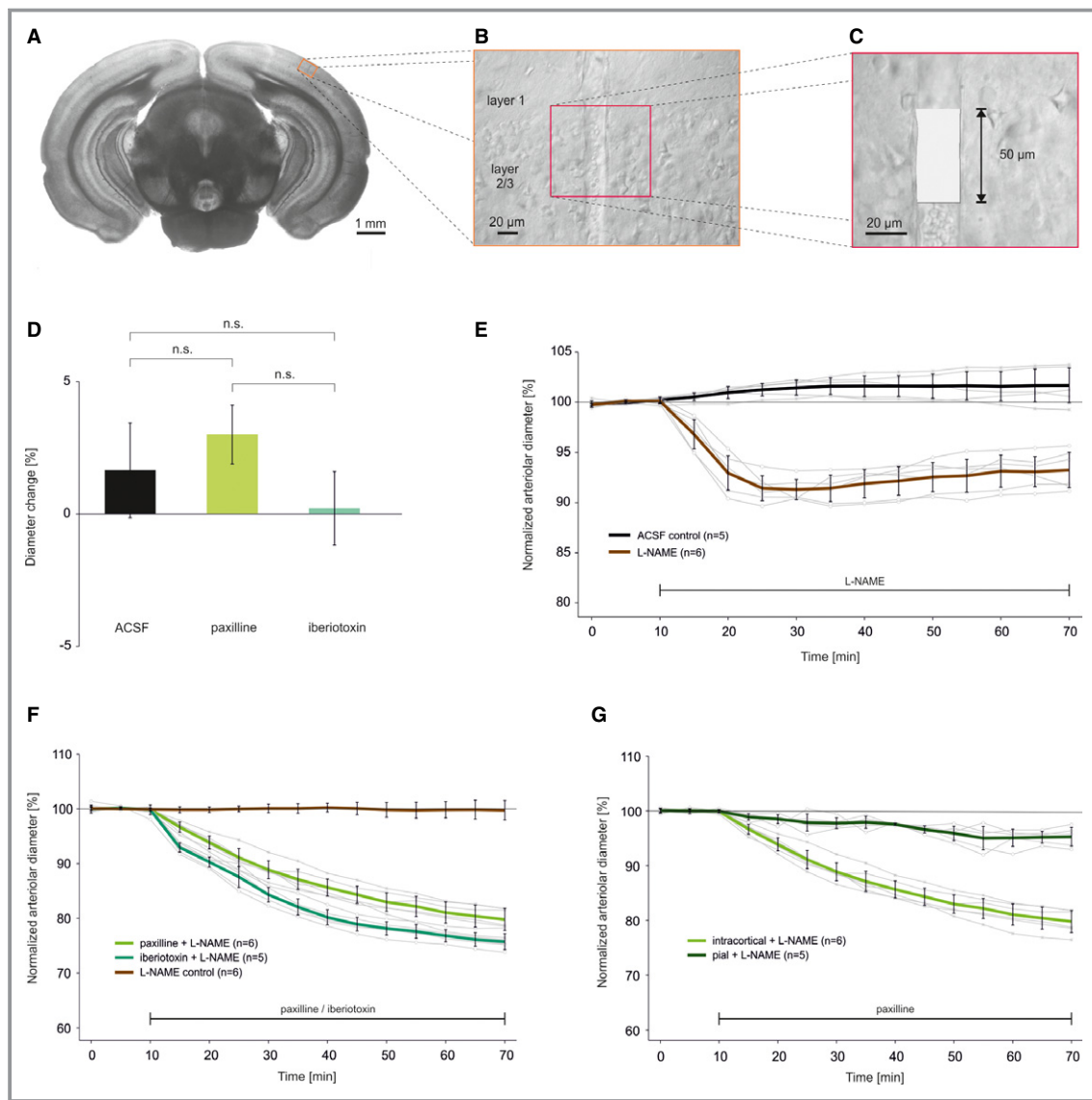
Data Quantification and Statistical Analysis

Data were gathered and evaluated using ImageJ (National Institutes of Health), Microsoft Excel, and OriginPro 8 (OriginLab). Because Kolmogorov–Smirnov tests indicated that data followed normal distribution, statistical analyses were determined using 1-way ANOVA with the Tukey test as post hoc analysis or Student *t* test. The parameter "n" represents the number of brain slices tested. Because only 1 arteriole per slice was always monitored, "n" also represents the number of arterioles. All values are presented as mean±SD. A value of $P \leq 0.05$ was considered statistically significant.

Results

Paxilline or Iberiotoxin Application Remain Ineffective on Vessel Diameter Change of Nonpreconstricted Arterioles

In a first set of experiments, we tested the stability of arteriole diameter in acute brain slices of mouse visual cortex during control conditions. In the absence of any drug administration and during 60 minutes of perfusion with aCSF control solution, no significant change in vessel diameter compared with baseline (1.6±1.8%; n=5 from 4 animals; *P*=0.11; 1-sample t test; Figure 1D) and no change in vessel wall width (data not shown) were observed. We conclude that, in our hands, video microscopy of arterioles in acute brain slices is a stable model system and, therefore, is suitable for quantifying changes in arteriolar diameter in vitro up to 6 hours.

Figure 1. Vasoactive effects of the BK$_{Ca}$ channel inhibitors paxilline and iberiotoxin on intracerebral arterioles in the presence or absence of the NO synthase inhibitor L-NAME. A, Acute brain slice of the occipital cortex (scale bar, 1 mm). B and C, Differential interference contrast images of an arteriole in layer 2/3 of mouse visual cortex. Arteriolar internal diameter was calculated as an area between opposite vessels walls along the length of 50 μm (scale bar, 20 μm). D, Bar diagram shows the missing influence of the BK$_{Ca}$ channel blockers paxilline and iberiotoxin on resting diameter in nonpreconstricted arterioles. E, Time course of diameter changes of intracortical arterioles after application of L-NAME (100 μmol/L) in comparison to control. F, Time–dependent diameter change of preconstricted arterioles after application of paxilline (1.5 μmol/L) or iberiotoxin (50 nmol/L) compared with L-NAME control. G, Time course of diameter changes of preconstricted arterioles after application of paxilline (1.5 μmol/L) in pial arterioles at the surface of the brain compared with intraparenchymal arterioles (same data as shown in 1F). H, After 45 minutes, the vasoconstrictive effect of L-NAME as well as the additional vasoconstriction by paxilline were independent of the presence of TTX. I, Statistical analysis of the vasoconstrictive potency of the BK$_{Ca}$ channel blockers paxilline and iberiotoxin on resting diameter of preconstricted arterioles analyzed 70 minutes after application. ***$P<0.001$. aCSF indicates artificial cerebrospinal fluid solution; L-NAME, N_ω-nitro-L-arginine methyl ester hydrochloride; n.s., not significant.

To understand the influence of the BK$_{Ca}$ channel function in the development of delayed cerebral vasospasm, we tested the vasoactive effects of the selective BK$_{Ca}$ channel inhibitors paxilline and IbTX on the resting diameter of arterioles in our brain slice model. Compared with aCSF control condition, application of paxilline (1.5 μmol/L) did not result in any significant diameter change ($3\pm1.1\%$; n=5 from 4 animals; $P=0.62$; 1-way ANOVA; Figure 1D). In line, the application of IbTX (50 nmol/L) induced no significant change in vessel diameter after 60 minutes compared with baseline ($0.2\pm1.4\%$;
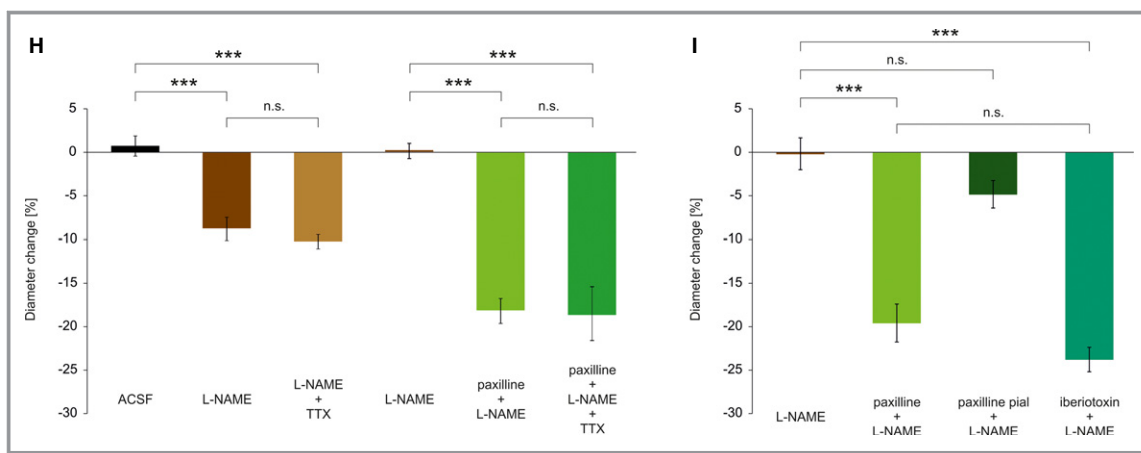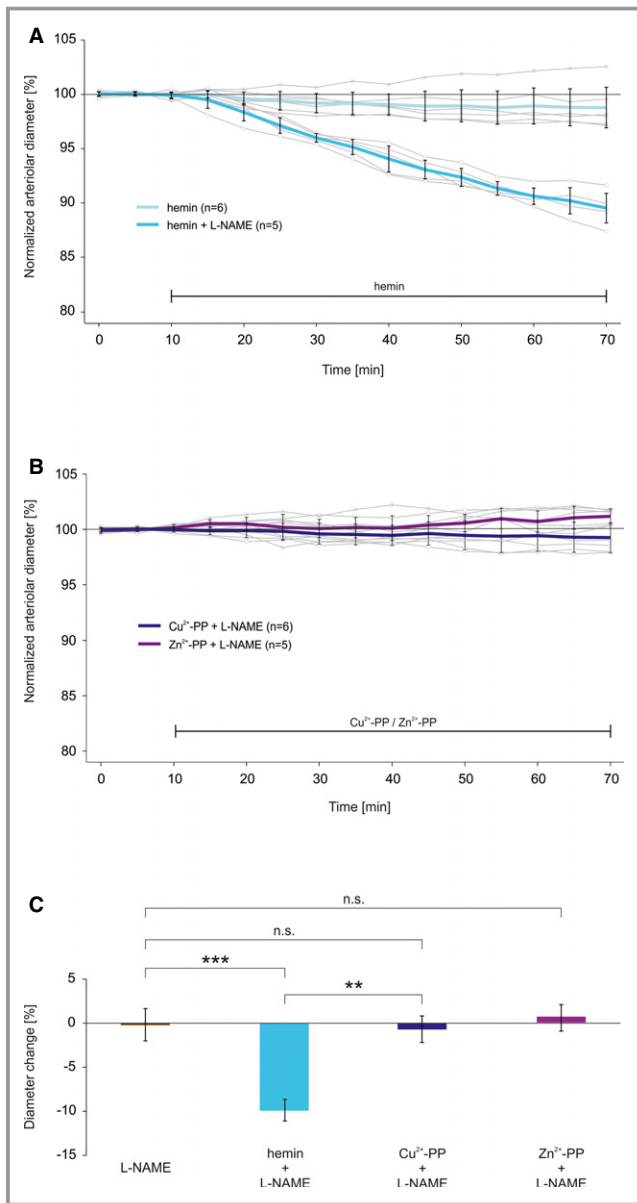
Figure 1. Continued.

n=5 from 3 animals; *P*=0.56: 1-way ANOVA; Figure 1D). Furthermore, the diameters of the paxilline and IbTX group were not statistically different (*P*=0.05). Collectively, these initial experiments demonstrated that the specific inhibition of BK_{Ca} channels did not alter vessel diameter significantly in nonpreconstricted intracerebral arterioles.

NO Synthase Inhibitor L-NAME Causes Increase in Arteriolar Tone

Our in vitro model is lacking intravascular blood pressure; therefore, in the absence of intact brain metabolism that includes blood flow autoregulation, the arterioles become relaxed. To mimic the myogenic tone of arterioles in vivo, we bath-applied L-NAME to prevent the generation of NO as one crucial vasodilative mediator. Antagonizing the NO-dependent signaling cascade, the application of L-NAME (100 µmol/L) constricted intracortical arterioles significantly by 6.8±1.7% (n=6 from 5 animals; *P*<0.001; 1-way ANOVA), and the vessel diameter reached a stable baseline 15 minutes after the wash-in (Figure 1E). Furthermore, experiments lasting 100 minutes confirmed the long-term stable vasoconstrictive effect of the NOS inhibitor (data not shown). Therefore, we concluded that the L-NAME-induced preconstriction is suitable for quantification of the vasoactive potency of BK_{Ca} channel-specific compounds, as described below. The NOS antagonist L-NAME also resulted in narrowing of the vascular lumen in the presence of tetrodotoxin (TTX) (0.5 µmol/L; n=5 from 4 animals; Figure 1H). This vasoconstrictive response was in the same order of magnitude as the preconstriction without TTX (*P*=0.27; 1-way ANOVA; Figure 1H). These data support the idea that the pretreatment of brain vessels with L-NAME increases vascular tone independent of voltage-sensitive sodium channel activity (eg, due to neuronal network activity).

Paxilline and Iberiotoxin Induce Vasoconstriction of Arterioles Pretreated With L-NAME

A substantial body of evidence had demonstrated that BK_{Ca} channels in astrocytic endfeet and VSMCs are involved in vasoregulation evoked by electrical field stimulation as well as under resting conditions.[17–19] If activated BK_{Ca} channels in VSMCs oppose vasoconstriction by membrane hyperpolarization in response to the increase in $[Ca^{2+}]_i$ following L-NAME application, BK_{Ca} channel inhibition should lead to VSMC membrane depolarization and hypertension. To investigate this hypothesis, we repeated our pharmacological experiments with the specific BK_{Ca} channel inhibitors by monitoring diameter changes on preconstricted vessels: 20 minutes after beginning the L-NAME incubation, we started the additional application of paxilline (1.5 µmol/L) or IbTX (50 nmol/L) for 60 minutes each. In contrast to the L-NAME application without previous preconstriction, paxilline (19.6 ± 2.2%; n=6 from 5 animals; *P*<0.001; 1-way ANOVA; Figure 1F) and IbTX (23.6±1.4%; n=5 from 5 animals; *P*<0.001; 1-way ANOVA; Figure 1F) induced prominent vasoconstriction without reaching a baseline. However, the diameter decrease in the paxilline group did not differ significantly from the IbTX group (*P*=0.65; Figure 1I). To test whether various types of arterioles show different ability to react, we compared the paxilline-induced decrease in diameter of intracortical arterioles in layer 2/3 with the responsiveness of pial arterioles located at the brain surface embedded in arachnoid membrane (n=5 from 4 animals). Interestingly, paxilline application induced a 4.8±1.6% vasoconstriction in pial arterioles that was significantly smaller than the vasoconstriction of layer 2/3 arterioles (*P*<0.001, 1-way ANOVA; Figure 1G). In addition, application of TTX (0.5 µmol/L) did not change the paxilline-dependent vasoconstriction in layer 2/3 arterioles significantly (n=5 from 4

Figure 2. Vasoactive impact of PPs on intracerebral arterioles preconstricted by L-NAME. A, Time course of diameter changes after application of hemin (1 μmol/L) in nonpreconstricted arterioles compared with arterioles preincubated with L-NAME. B, Time course of diameter changes of preconstricted arterioles after application of Cu^{2+}-PP (1 μmol/L) or Zn^{2+}-PP (1 μmol/L). C, Hemin acted as a specific vasoconstrictor in arterioles pretreated with L-NAME, whereas Cu^{2+}-PP and Zn^{2+}-PP failed to induce a vasoconstrictive effect in both preconstricted and nonpreconstricted vessels. **$P<0.01$; ***$P<0.001$. L-NAME indicates N_{ω}-nitro-L-arginine methyl ester hydrochloride; n.s., not significant; PP, protoporphyrin.
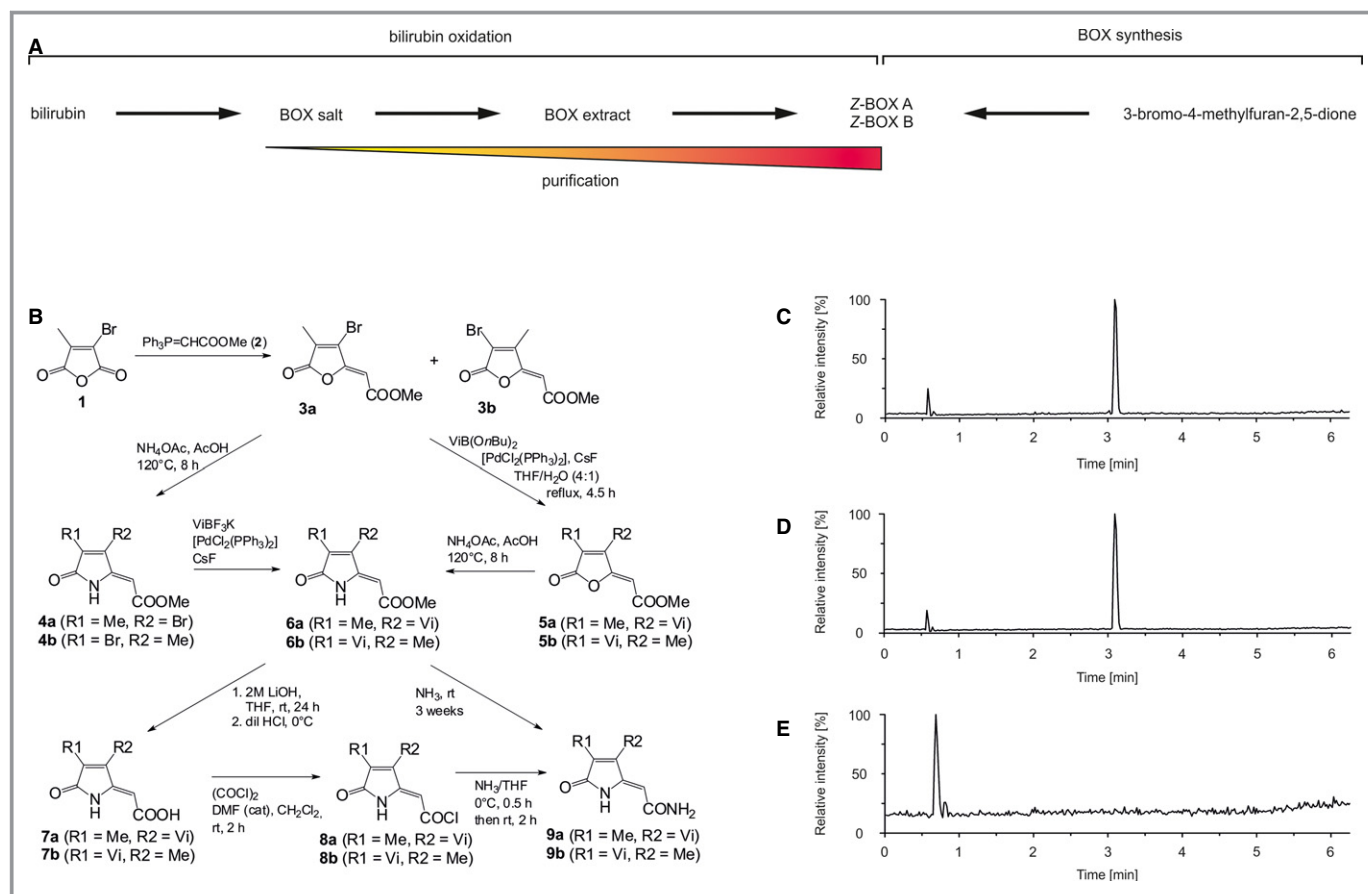
animals; $P=0.27$; 1-way ANOVA; Figure 1H). Taking these observations into consideration, we argue that the long-lasting vasospastic effect of paxilline is location dependent and appears to be independent of voltage-gated sodium channel function.

Hemin Acts as Specific Vasoconstrictor in Preconstricted Arterioles

To further evaluate the specificity and the potential contribution of heme to delayed vasospasm after subarachnoid hemorrhage, we tested the vasoactivity of 3 types of metalloprotoporphyrin IX: Zn^{2+}-PP, Cu^{2+}-PP, and hemin. In case of arterioles not pretreated with L-NAME, a 60-minute application of hemin (1 μmol/L) resulted in a small vasoconstriction of 1.2±1.9% (n=6 from 4 animals; $P<0.05$; 1-way ANOVA; Figure 2A) in comparison to the aCSF control group. Application of Cu^{2+}-PP (1 μmol/L) led to no significant change in vessel diameter compared with control conditions (1.4±0.9%; n=5 from 3 animals; $P=1$; 1-way ANOVA; data not shown). In contrast, Zn^{2+}-PP (1 μmol/L) induced a prominent increase in diameter up to 12.2 ± 1.8% (n=5 from 3 animals; $P<0.001$). Arteriolar preconstriction with L-NAME converted the hemin-induced small vasoconstriction into a progressive and significant diameter decrease of 9.9±1.2% after 60 minutes (n=5 from 5 animals; $P<0.001$; Figure 2A and 2C). Different from hemin, the vasoconstrictive effect on arteriolar diameter failed to appear in preconstricted vessels after bath application of Cu^{2+}-PP (−0.7±1.5%; n=6 from 5 animals; $P=1$; Figure 2B and 2C) or Zn^{2+}-PP (1.0±1.0%; n=5 from 4 animals; $P=1$; Figure 2B and 2C). The finding that iron-containing protoporphyrin acted as a specific vasoconstrictor in preconstricted arterioles supports the assumption that the iron center of hemin or its charge determines its ability to alter vascular tone.[13,20]

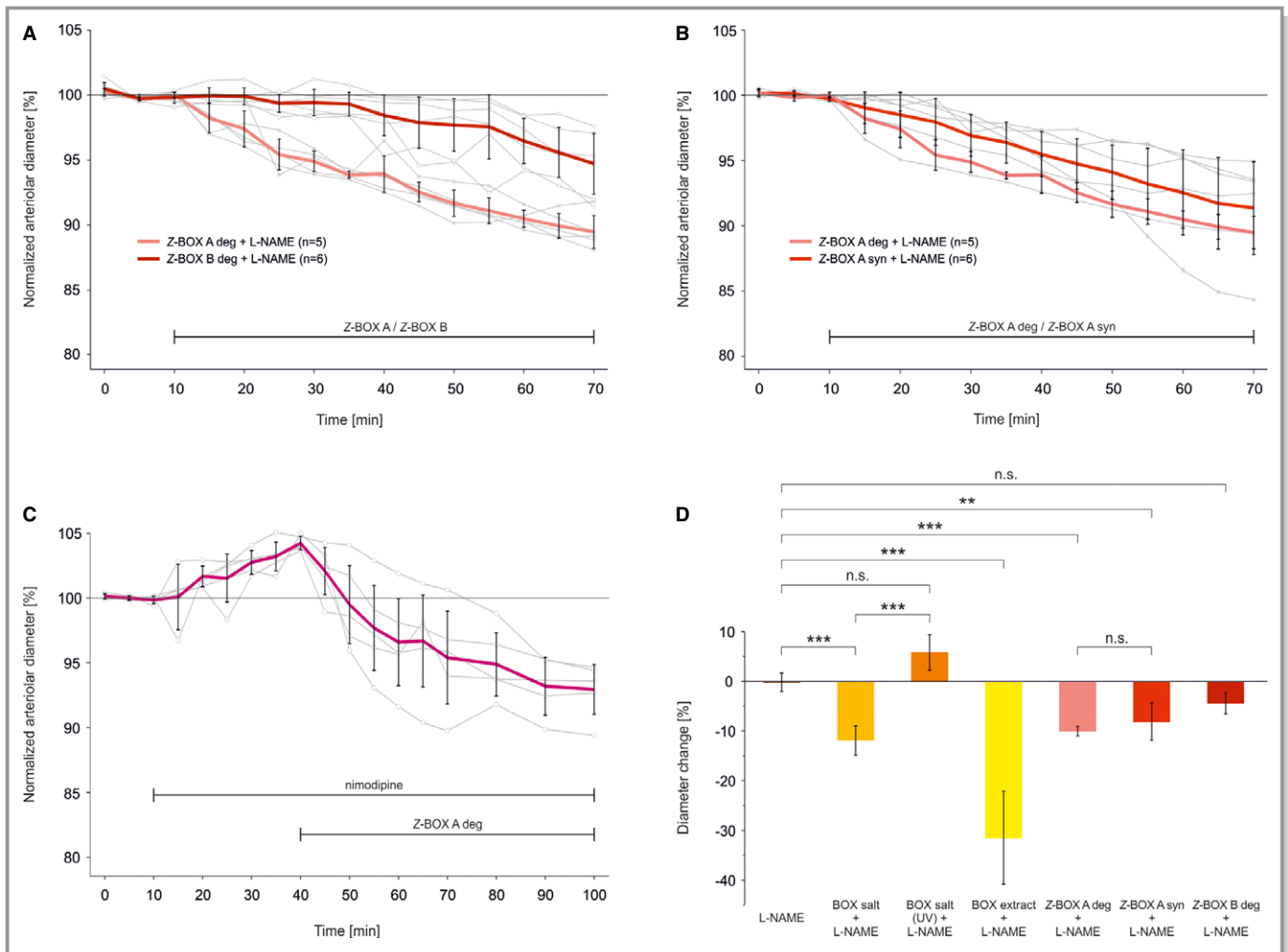## BOX-Containing Mixtures and BOX Isomers Decrease Arteriolar Diameter

The concentration increase of BOXes surrounding perivascular hematoma in post-SAH patients and the presence of free radicals from inflammatory cell metabolism are considered to be major mediators of vasospasm induction.[5,7] In a subset of experiments on preconstricted arterioles, we examined the vasoactivity of BOX-containing preparations of the oxidative bilirubin degradation process[4] and the purified isomers Z-BOX A and Z-BOX B (Figure 3A). BOX salt, the crude mixture of the oxidative in vitro degradation of bilirubin, dissolved in L-NAME-containing aCSF solution at a final concentration of 1 mg/mL, caused significant vasoconstriction of 11.9±3.0% in preconstricted arterioles (n=6 from 6 animals; $P<0.001$; 1-way ANOVA; Figure 4D). Ultraviolet light–exposed BOX salt solution (254 nm for 5 hours) was not effective in inducing vasoconstriction and converted the response to a nonsignificant increase in vascular diameter (5.8±3.5%; n=5 from 5 animals; $P=0.14$; 1-way ANOVA; Figure 4D), confirming that BOXes lose their biological activity by isomerization or degradation after illumination in the ultraviolet range.[12,15] In a next step of compound purification, we determined changes

Figure 3. Preparation of BOX–containing treatments via oxidative bilirubin degradation or chemical synthesis. A, Scheme of purification steps in the preparation of BOX-containing treatments via bilirubin degradation or chemical synthesis. B, Selective synthesis of the pure isomers Z-BOX A (9a) and Z-BOX B (9b) in 4 to 6 steps beginning from 3-bromo-4-methylfurane–2,5-dione (1). C–E, Postexperimental analysis via ultra-performance liquid chromatography coupled to time-of-flight mass spectrometry proves substance identity as well as comparable concentration and purity of the applied Z-BOX A treatments. Base peak intensity plots of Z-BOX A (peak at 3.1 minutes) in artificial cerebrospinal fluid solution from bilirubin oxidation procedure (C) and from synthesis (D) compared with blank measurement that contains only the injection peak (E). Ac indicates acetyl; Bu, butyl; Me, methyl; Ph, phenyl; THF, tetrahydrofuran; Vi, vinyl; Z-BOX A, Z-isomer of BOX A.

in arteriolar diameter after application of BOX extract (0.03 mg/mL), generated from the dried chloroform extract of the salt mixture. BOX extract induced a substantial decrease in vessel diameter by $31.5 \pm 9.4\%$ (n=5 from 4 animals; $P<0.001$; 1-way ANOVA; Figure 4D) within 15 minutes. A 30-minute–long washout of BOX extract did not lead to any significant change in vessel diameter (31.5% to 28.4% compared with baseline; n=5 from 4 animals), indicating the long-lasting vasospastic effect of oxidized species of bilirubin. To evaluate the vasoactive impact of single isomers obtained from oxidative bilirubin degradation, we bath-applied 5 μmol/L of the purified isomers Z-BOX A or Z-BOX B (referred to as "Z-BOX A deg" and "Z-BOX B deg," respectively), which differ from each other only by the switched positions of their vinyl and methyl groups (Figure 3B). Z-BOX A deg affected the diameter of preconstricted arterioles significantly by $10.0\pm0.9\%$ vaso-constriction (n=5 from 4 animals; $P<0.001$; 1-way ANOVA). In contrast, Z-BOX B deg at the same concentration induced

smaller vasoconstriction of $4.4\pm2.2\%$ (n=6 from 4 animals), which was not significantly different compared with the L-NAME control group ($P=0.57$; 1-way ANOVA; Figure 4A). To exclude an epiphenomenon caused by contaminants from the degradation of bilirubin, we investigated whether synthetically generated Z-BOX A provokes constrictive vascular effects similar to those that occurred after application of Z-BOX A deg obtained from oxidative bilirubin degradation. To verify the identical structure of Z-BOX A isomers in these preparations, we analyzed the compounds with nuclear magnetic resonance spectroscopy and compared the purity and content of the isomer postexperimentally with UPLC coupled to mass spectrometry (Figure 3C through 3E). Corresponding to these aspects, both preparations were chemically equivalent. No significant differences were found, indicating that a relevant product from bilirubin degradation is Z-BOX A. The application of synthetic Z-BOX A (5 μmol/L) resulted in a significant continuous narrowing of the arteriolar lumen ($8.1\pm3.8\%$; n=6

Figure 4. Vasoconstrictive effect of BOX-containing compounds on intracerebral arterioles preconstricted by L-NAME. A, Time course of diameter changes of preconstricted arterioles after application of *Z*-BOX A deg (5 µmol/L) or *Z*-BOX B deg (5 µmol/L). B, Time course of diameter changes of preconstricted arterioles after application of *Z*-BOX A deg (5 µmol/L) in comparison to *Z*-BOX A syn (5 µmol/L). C, Time course of diameter changes of preconstricted arterioles after *Z*-BOX A deg (5 µmol/L) application in the presence of nimodipine (1 mmol/L). D, Statistical analysis of vasoconstrictive potency of different BOX preparations in preconstricted arterioles. **P< 0.01; ***P< 0.001. BOX indicates bilirubin oxidation; deg, derived from bilirubin degradation; L-NAME N_ω-nitro-L-arginine methyl ester hydrochloride; n.s., not significant; syn, derived from chemical synthesis; UV, ultraviolet; *Z*-BOX A, *Z*-isomer of BOX A.

from 5 animals; *P*<0.01; Figure 4B). During the observation period, the amplitude of vasoconstriction did not differ significantly from the results obtained with *Z*-BOX A deg (*P*=1; 1-way ANOVA; Figure 4B and 4D). To quantify the stability of *Z*-BOX A syn during the experiment, we used HPLC–tandem mass spectrometry analysis and determined the relative concentration of *Z*-BOX A syn in samples of aCSF solution before and after the experiments. The results show no significant degradation of *Z*-BOX A syn during the experiment (97.4±10.6% of original concentration; *t* test; *P*=0.81; n=7).

Currently, nimodipine is the primary pharmacological intervention recommended as prophylaxis against cerebral vasospasm.[21] To investigate the vasoactivity of the potent L-type calcium channel inhibitor, we bath-applied 1 mmol/L nimodipine on preconstricted arterioles. After 30 minutes,

vessel diameter increased up to 104±0.5% in comparison to the baseline level (n=5 from 5 animals; Figure 4C). The additional application of *Z*-BOX A deg (5 µmol/L) reversed the small vasodilation in a significant vasoconstriction to 93±1.9% (n=5 from 5 animals; *P*<0.001; 1-way ANOVA; Figure 4C) of the initial diameter.

Paxilline and *Z*-BOX A Remain Ineffective on Vascular Diameter in Acute Brain Slices from Slo1$^{-/-}$ Animals

To estimate the impact of calcium-activated BK$_{Ca}$ potassium channels on BOX-induced vessel constriction, we evaluated the effect of arteriolar vasoactivity of *Z*-BOX A deg in mice lacking the pore-forming α-subunit of BK$_{Ca}$ channels[22] (kindly

provided by Toshinori Hoshi, Philadelphia, PA). Under control conditions, all arterioles (n_{slices}=20; $n_{animals}$=11) selected for diameter analysis showed an increased vascular tone after preincubation with L-NAME, indicated by significantly thicker vessel wall and smaller vessel diameter (P<0.01; data not shown). In contrast to the series of experiments in C57BL/6J mice, in brain slices of Slo1$^{-/-}$ mice, no significant diameter change could be observed with application of paxilline (1.5 µmol/L) for more than 60 minutes. The weak vasoconstriction of 1.4±0.9% did not differ significantly from the L-NAME control group (n=5 from 3 animals; P=0.7; 1-way-ANOVA; Figure 5B and 5E). To reinforce this result, we bath-applied Z-BOX A deg (5 µmol/L) and, again, did not observe any significant diameter change in preconstricted arterioles in slices of Slo1$^{-/-}$ animals (0.2±1.4%; n=5 from 2 animals; P=0.63; 1-way ANOVA; Figure 5C and 5E). Finally, we examined whether synthetic Z-BOX A has an impact on arteriolar vessel diameter in brain slices of Slo1$^{-/-}$ animals. In line with the results using Z-BOX A deg, Z-BOX A syn failed to induce vasoconstriction in comparison to the L-NAME control group (0.6±1.4%; n=5 from 4 animals; P=0.37; 1-way ANOVA; Figure 5D and 5E). We conclude that the vasoconstrictive potency of paxilline as well as Z-BOX A depend on the presence of BK$_{Ca}$ potassium channels.

Our data demonstrate for the first time that individual heme degradation products cause significant vasoconstriction in cerebral arterioles that is mediated by BK$_{Ca}$ channel activity but that, at the same time, differ in their vasoactive potency.
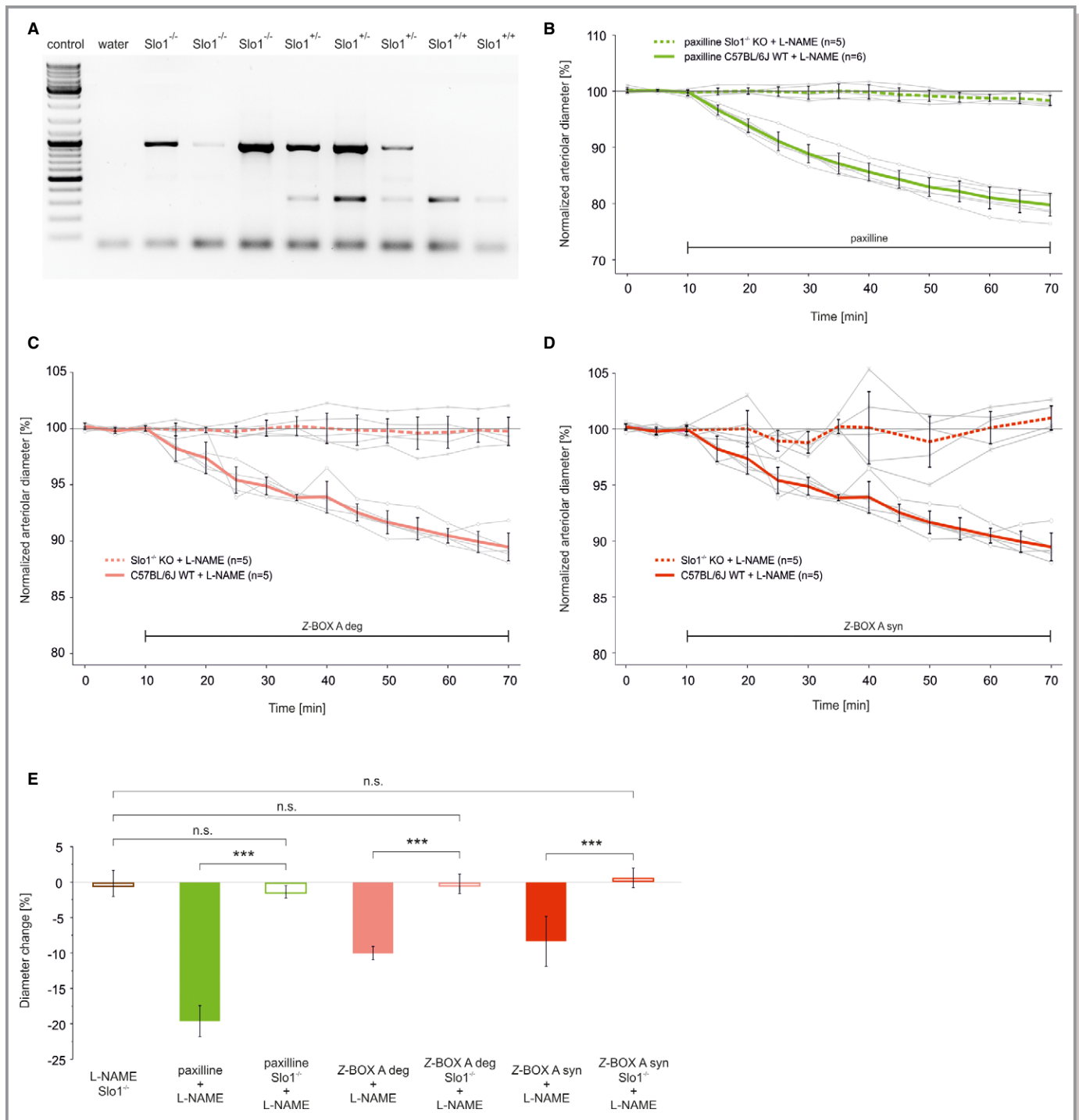
Discussion

Delayed cerebral vasospasm causing death or severe neurological deficits is one of the major complications in patients who survive subarachnoid hemorrhage. Previous studies suggest that the products of oxidative hemoglobin degradation might be responsible for the irreversible vasoconstriction. So far, only mixtures of bilirubin degradation products have been tested in animal models for their vasoactive propensity. Using an in vitro model of cerebral vasodiameter, a central finding of this study is that heme alone and individual heme degradation products including different BOXes species induce long-lasting vasoconstriction in cerebral arterioles. The vasoconstrictive effect was detected only if arterioles were preconstricted using the NOS inhibitor L-NAME. Because arterioles become relaxed in brain slices missing intravascular blood pressure and autoregulation, this pharmacological pretreatment enabled us to simulate the physiological resting tone present in vivo. The L-NAME–based preconstriction is in line with the hypothesis that, under physiological conditions, the resting tone activates stretch-activated cation channels in VSMCs that are counter-

acted by BK$_{Ca}$ channel activation.[23,24] Inhibition of BK$_{Ca}$ channel conductivity by heme or BOXes would lead to more depolarized membrane potentials and, therefore, would induce further smooth muscle cell contraction. Besides thromboxane A2 receptor agonists (eg, U46619) or prostaglandin F2α, various studies have used L-NAME as an agent for simulation and perpetuation of vascular tone.[25–27] Preincubation of brain slices with the unspecific NOS inhibitor L-NAME increases [Ca^{2+}]$_i$ in VSMCs by both the decrease of basal NO release by inhibition the constitutive neuronal NOS[28] and by the down-regulation of protein kinase G signaling pathways.[29] Under physiological conditions, protein kinase G induces activation of myosin light chain phosphatase,[30] inhibits calcium release from the sarcoplasmatic reticulum mediated by inositol trisphosphate receptors,[31] and increases the cellular potassium efflux by BK$_{Ca}$ channel phosphorylation.[32] In our hands, after antagonizing these NO-related vasodilative mechanisms, arteriole diameter decreased to near 90% of the initial diameter in vitro (Figure 1E). Consequently, this partial vasoconstriction would allow the detection of an additional decrease as well as of an increase in arteriolar diameter due to any additional pharmacological application.

In accordance with the postulated molecular mechanism of blocking BK$_{Ca}$ channel conductance by hemoglobin degradation products, similar effects could be obtained by application of the specific BK$_{Ca}$ channel blockers IbTX or paxilline. Suppression of potassium efflux owing to blockade Slo1 S6 helix in case of paxilline,[33] binding the outer vestibule of the channel pore by IbTX,[34] or interaction with the linker sequence between S6 helix and the RCK1 domain in the case of BOXes are not supposed to restrict the open probability of voltage-dependent calcium channels and, therefore, would increase global [Ca^{2+}]$_i$ mediated on membrane depolarization.

Even though pial and intraparenchymal vessels possess structural and functional similarities, the paxilline-induced diameter decrease in arterioles located at the pial surface was significantly lower than in arterioles of equal size located at the transition to layer 2/3 at a cortical depth of roughly 150 µm (Figure 1G and 1I). At first glance, this finding supports the hypothesis that the interaction of vascular muscle cells with the perivascular neuronal network explains the different vasoreactivity because, different from pial vessels, intraparenchymal arterioles and encircling astrocytic endfeet form a neurovascular unit.[18,25,35] This assumption was challenged because the vasoconstrictive effect of paxilline was still present after application of the sodium channel blocker TTX and, therefore, was independent of neuronal activity (Figure 1H). In addition, it has been shown previously that intraparenchymal arterioles generate a significantly stronger pressure-induced myogenic tone than pial arterioles.[36] Furthermore, at constant intravascular pressure, electrophys-

Figure 5. Paxilline and *Z*-BOX A failed to induce vasoconstriction in arterioles of Slo1$^{-/-}$ mice. A, Exemplary genotyping of Slo1 littermates by polymerase chain reaction analysis of tail biopsies. Signals of the WT band (332 bp) or the KO band (1000 bp) enable the identification of homozygote or heterozygote genotypes. B, Time course of diameter changes of preconstricted arterioles in Slo1$^{-/-}$ mice after application of paxilline (1.5 μmol/L). C, Time course of diameter changes of preconstricted arterioles in Slo1$^{-/-}$ mice after application of *Z*-BOX A deg (5 μmol/L). D, Time course of diameter changes of preconstricted arterioles in Slo1$^{-/-}$ mice after application of *Z*-BOX A syn (5 μmol/L) in comparison to C57BL/6J WT mice. E, Statistical analysis of the vasoactive potency of paxilline and *Z*-BOX A obtained from oxidative bilirubin degradation and from synthesis on preconstricted arterioles in Slo1-deficient mice compared with WT C57BL/6J mice. ***$P < 0.001$. BOX A indicates *Z*-isomer of BOX A; deg, derived from bilirubin degradation; L-NAME indicates N_ω-nitro-L-arginine methyl ester hydrochloride; KO, knockout; n.s., not significant; syn, derived from chemical synthesis; WT, wild type.

iological measurements in muscle cells of arterioles in layer 2/3 demonstrated stronger depolarization with higher $[Ca^{2+}]_i$ than VSMCs of arterioles at the brain surface.[37] Further investigations are required to determine whether the location-dependent effect of paxilline results in different BK_{Ca} densities along arterial vascular segments.

To identify individual compounds of hemoglobin degradation products, we first examined the impact of 3 metal protoporphyrins on arteriolar diameter. In accordance with previous investigations from Tang et al, who have shown the inhibitory action of hemin on BK_{Ca} channel current amplitude,[13] bath application of hemin caused progressive diameter decrease in preconstricted arterioles (Figure 2A), whereas Zn^{2+} protoporphyrin and Cu^{2+} protoporphyrin did not alter the width of arterioles. The hemin-specific regulation of BK_{Ca} channel function is primarily mediated by the CKACH binding motif located between the intracellular RCK domains. Consequently, mutations of cysteine and histidine residues in the sequence CKACH eliminated the hemin sensitivity of BK_{Ca} channels.[13,38] Further investigations revealed that hemin-mediated inhibition of BK_{Ca} channels correlates with the increase in cytosolic calcium concentration.[20] These characteristics provide a possible explanation of why L-NAME preincubation of brain slices and subsequent inhibition of PKG signal pathways strengthen the vasoconstrictive effect of hemin.

To trace back the vasoconstrictive activity of heme and heme degradation products to single chemical compounds, we tested three different preparations of BOXes in our in vitro model. The unpurified freeze-dried crude bilirubin oxidation mixture, BOX salt, consists (aside from small amounts of *Z*-BOX A and *Z*-BOX B) of numerous inorganic and organic compounds that might feature vasoactive potential. The observed vasoconstrictive effect of BOX salt can result from the additive or subtractive effects of single vasoactive compounds or due to synergistic interplays. In particular, traces of peroxides—that remain in the freeze-drying step of oxidative bilirubin degradation—can directly influence the vascular diameter by acting as substrates of signaling cascades or via modulation of redox states that switch or interrupt signaling pathways. The loss of vasoconstrictive properties after ultraviolet irradiation of BOX salt is controversial. Following the recent findings that, like bilirubin, particular products from bilirubin breakdown are able to undergo photoisomerization,[14] light-induced structural changes in the conformation of double bonds of vasoactive compounds seem possible. This would lead to a decrease in the primary compounds and would explain the mitigation of the vasoconstrictive effect.

The very strong vasoconstrictive effect observed after application of BOX salt's contained nonpolar substances (BOX extract) is in line with the concentration increase of vasoac-

tive compounds due to the extraction with chloroform. In both HPLC-purified single-compound treatments, *Z*-BOX A and *Z*-BOX B, peroxide activity could not be detected.

Z-BOX A, purified from oxidative bilirubin degradation, showed a vasoconstrictive effect similar to that of hemin. Interestingly, the vasoconstrictive potency of the regio-isomer *Z*-BOX B was significantly weaker. Although the time course of vasoconstriction after *Z*-BOX B administration was slower at first compared with the time course of *Z*-BOX A–induced vasoconstriction, we cannot exclude that, for longer administration times, both compounds would cause similar effects. Whether both isomers aggregate their vasoconstrictive effects or behave competitively must be the subject of future studies. Nevertheless, because the potential binding site for both isomers is supposed to be equivalent, the difference in vasoactive effect could be a starting point for the development of a chemical compound that occupies the binding site at the BK_{Ca} channel without having the inhibitory effect of different BOXes species.

Besides "triple-H therapy" and the clinical management of intracranial pressure, treatment with the calcium channel antagonist nimodipine is the main approved pharmacological intervention for patients suffering from cerebral hemorrhage.[21] Although sound data indicating a significant benefit of this treatment are still missing, no alternative therapy based on direct modulation of ion channel activity is available. In accordance, application of nimodipine in our in vitro model did not prevent the vasoconstrictive effect of *Z*-BOX A. Although nimodipine alone already showed vasodilatative potency, the additional application of *Z*-BOX A yielded similar relative vasoconstriction compared with control.

To exclude potential contamination of purified *Z*-BOX A originated from oxidative degradation with unknown vasoactive compounds, we synthesized *Z*-BOX A with chemical means from scratch (*Z*-BOX A syn).[16] Both batches of *Z*-BOX A, one originated from oxidative degradation the other from chemical synthesis, showed similar vasoconstrictive effects. Consequently, we can exclude contamination of *Z*-BOX A originated from the degradation process with unknown vasoactive compounds from responsibility for the observed vasoconstrictive effect of *Z*-BOX A.

To pinpoint the vasoconstrictive effect of *Z*-BOX A on its postulated molecular target, the inhibition of BK_{Ca} channel conductivity, we applied paxilline and *Z*-BOX A to acute brain slices of mice lacking the BK_{Ca} channel α-subunits. Before the pharmacological incubation began, the morphometric analyses of vessels showed that the inner and outer diameters of intracortical arterioles were already statistically significantly smaller than the arteriolar diameter of C57BL6/J mice (data not shown). These observations support the idea that the decrease in diameter of intracortical arterioles reflects the loss of hyperpolarized potassium efflux in VSMCs. In line with

this hypothesis, previous studies found that Slo1$^{-/-}$ mice had higher systemic blood pressure than Slo1$^{+/+}$ mice due to reduced frequencies in spontaneous transient outward potassium currents in vascular muscle cells[39] and hyperaldosteronism.[40] Neither the administration of paxilline nor the administration of Z-BOX A induced any significant change in arteriole diameter compared with baseline in slices of Slo1-deficient mice. In addition, this was true for both Z-BOX A types, whether originated from oxidative bilirubin degradation or chemical synthesis. Consequently, we conclude that the vasoconstrictive effect of Z-BOX A is mediated by a change in BK$_{Ca}$ channel conductivity.

In conclusion, we identified individual components of the oxidative bilirubin degradation process that lead to vasoconstriction of cerebral arterioles mediated by BK$_{Ca}$ channel activity. Although the confirmation of our data by an in vivo SAH model is still missing and the means by which heme and heme degradation products get into the cortex after SAH is unclear, the vasoconstrictive effect might represent a signaling pathway in the occurrence of delayed cerebral vasospasm in subarachnoid hemorrhage patients. In addition, the different vasoactive potency of the regio-isomers Z-BOX A and Z-BOX B on intracortical arterioles has not been documented previously and improves understanding of the pathogenesis of cerebral vasospasm following subarachnoid hemorrhage.

Acknowledgments

Sources of Funding

Disclosures

None.

References

1. Huang J, van Gelder JM. The probability of sudden death from rupture of intracranial aneurysms: a meta-analysis. *Neurosurgery*. 2002;51:1101–1105.

2. Loftspring MC, Wurster WL, Pyne-Geithman GJ, Clark JF. An in vitro model of aneurysmal subarachnoid hemorrhage: oxidation of unconjugated bilirubin by cytochrome oxidase. *J Neurochem*. 2007;102:1990–1995.

3. Macdonald RL, Pluta RM, Zhang JH. Cerebral vasospasm after subarachnoid hemorrhage: the emerging revolution. *Nat Clin Pract Neurol*. 2007;3:256–263.

4. Kranc KR, Pyne GJ, Tao L, Claridge TD, Harris DA, Cadoux-Hudson TA, Turnbull JJ, Schofield CJ, Clark JF. Oxidative degradation of bilirubin produces vasoactive compounds. *Eur J Biochem*. 2000;267:7094–7101.

5. Clark JF, Reilly M, Sharp FR. Oxidation of bilirubin produces compounds that cause prolonged vasospasm of rat cerebral vessels: a contributor to subarachnoid hemorrhage-induced vasospasm. *J Cereb Blood Flow Metab*. 2002;22:472–478.

6. Pyne-Geithman GJ, Morgan CJ, Wagner K, Dulaney EM, Carrozzella J, Kanter DS, Zuccarello M, Clark JF. Bilirubin production and oxidation in CSF of patients with cerebral vasospasm after subarachnoid hemorrhage. *J Cereb Blood Flow Metab*. 2005;25:1070–1077.

7. Clark JF, Sharp FR. Bilirubin oxidation products (BOXes) and their role in cerebral vasospasm after subarachnoid hemorrhage. *J Cereb Blood Flow Metab*. 2006;26:1223–1233.

8. Clark JF, Loftspring M, Wurster WL, Beiler S, Beiler C, Wagner KR, Pyne-Geithman GJ. Bilirubin oxidation products, oxidative stress, and intracerebral hemorrhage. *Acta Neurochir Suppl*. 2008;105:7–12.

9. Sharp FR, Massa SM, Swanson RA. Heat-shock protein protection. *Trends Neurosci*. 1999;22:97–99.

10. Ledoux J, Werner ME, Brayden JE, Nelson MT. Calcium-activated potassium channels and the regulation of vascular tone. *Physiology*. 2006;21:69–78.

11. Hou S, Heinemann SH, Hoshi T. Modulation of BKCa channel gating by endogenous signaling molecules. *Physiology (Bethesda)*. 2009;24:26–35.

12. Hou S, Xu R, Clark JF, Wurster WL, Heinemann SH, Hoshi T. Bilirubin oxidation end products directly alter K+ channels important in the regulation of vascular tone. *J Cereb Blood Flow Metab*. 2011;31:102–112.

13. Tang XD, Xu R, Reynolds MF, Garcia ML, Heinemann SH, Hoshi T. Haem can bind to and inhibit mammalian calcium-dependent Slo1 BK channels. *Nature*. 2003;425:531–535.

14. Friedrich B, Mueller F, Feiler S, Scholler K, Plesnila N. Experimental subarachnoid hemorrhage causes early and long-lasting microarterial constriction and microthrombosis: an in-vivo microscopy study. *J Cereb Blood Flow Metab*. 2012;32:447–455.

15. Wurster WL, Pyne-Geithman GJ, Peat IR, Clark JF. Bilirubin oxidation products (BOXes): synthesis, stability and chemical characteristics. *Acta Neurochir Suppl*. 2008;104:43–50.

16. Klopfleisch M, Seidel RA, Goerls H, Richter H, Beckert R, Imhof W, Reiher M, Pohnert G, Westerhausen M. Total synthesis and detection of the bilirubin oxidation product (z)-2-(3-ethenyl-4-methyl-5-oxo-1,5-dihydro-2 h-pyrrol-2-ylidene)ethanamide (z-box a). *Org Lett*. 2013;15:4608–4611.

17. Loehn M, Lauterbach B, Haller H, Pongs O, Luft FC, Gollasch M. Beta(1)-subunit of BK channels regulates arterial wall[Ca^{2+})] and diameter in mouse cerebral arteries. *J Appl Physiol*. 2001;91:1350–1354.

18. Girouard H, Bonev AD, Hannah RM, Meredith A, Aldrich RW, Nelson MT. Astrocytic endfoot Ca^{2+} and BK channels determine both arteriolar dilation and constriction. *Proc Natl Acad Sci USA*. 2010;107:3811–3816.

19. Koide M, Bonev AD, Nelson MT, Wellman GC. Inversion of neurovascular coupling by subarachnoid blood depends on large-conductance Ca^{2+}-activated K$^+$ (BK) channels. *Proc Natl Acad Sci USA*. 2012;109:E1387–E1395.

20. Horrigan FT, Heinemann SH, Hoshi T. Heme regulates allosteric activation of the slo1 BK channel. *J Gen Physiol*. 2005;126:7–21.

21. Rinkel GJ, Feigin VL, Algra A, Van den Bergh WM, Vermeulen M, Van Gijn J. Calcium antagonists for aneurysmal subarachnoid haemorrhage. *Cochrane Database Sys Rev*. 2005; (1):CD000277.

22. Meredith AL, Thorneloe KS, Werner ME, Nelson MT, Aldrich RW. Overactive bladder and incontinence in the absence of the BK large conductance Ca^{2+}-activated K$^+$ channel. *J Biol Chem*. 2004;279:36746–36752.

23. Kirber MT, Walsh JV Jr, Singer JJ. Stretch-activated ion channels in smooth muscle: a mechanism for the initiation of stretch-induced contraction. *Eur J Physiol*. 1988;412:339–345.

24. Zou H, Lifshitz LM, Tuft RA, Fogarty KE, Singer JJ. Visualization of Ca^{2+} entry through single stretch-activated cation channels. *Proc Natl Acad Sci USA*. 2002;99:6404–6409.

25. Gordon GR, Mulligan SJ, MacVicar BA. Astrocyte control of the cerebrovasculature. *Glia*. 2007;55:1214–1221.

26. Govindaraju V, Teoh H, Hamid Q, Cernacek P, Ward ME. Interaction between endothelial heme oxygenase-2 and endothelin-1 in altered aortic reactivity after hypoxia in rats. *Am J Physiol Heart Circ Physiol*. 2005;288:H962–H970.

27. Zonta M, Angulo MC, Gobbo S, Rosengarten B, Hossmann KA, Pozzan T, Carmignoto G. Neuron-to-astrocyte signaling is central to the dynamic control of brain microcirculation. *Nat Neurosc*. 2003;6:43–50.

28. Furfine ES, Carbine K, Bunker S, Tanoury G, Harmon M, Laubach V, Sherman P. Potent inhibition of human neuronal nitric oxide synthase by N(G)-nitro-L-arginine methyl ester results from contaminating N(G)-nitro-L-arginine. *Life Sci*. 1997;60:1803–1809.

29. Boeger RH, Bode-Boeger SM, Gerecke U, Frolich JC. Long-term administration of L-arginine, L-NAME, and the exogenous NO donor molsidomine modulates urinary nitrate and cGMP excretion in rats. *Cardiovasc Res*. 1994;28:494–499.

30. Nakamura K, Koga Y, Sakai H, Homma K, Ikebe M. cGMP-dependent relaxation of smooth muscle is coupled with the change in the phosphorylation of myosin phosphatase. *Circ Res*. 2007;101:712–722.

31. Schlossmann J, Ammendola A, Ashman K, Zong X, Huber A, Neubauer G, Wang GX, Allescher HD, Korth M, Wilm M, Hofmann F, Ruth P. Regulation of intracellular calcium by a signalling complex of IRAG, IP3 receptor and cGMP kinase Ibeta. *Nature*. 2000;404:197–201.

32. Fukao M, Mason HS, Britton FC, Kenyon JL, Horowitz B, Keef KD. Cyclic GMP-dependent protein kinase activates cloned BKCa channels expressed in mammalian cells by direct phosphorylation at serine 1072. *J Biol Chem*. 1999;274:10927–10935.

33. Zhou Y, Tang QY, Xia XM, Lingle CJ. Glycine311, a determinant of paxilline block in BK channels: a novel bend in the BK s6 helix. *J Gen Physiol*. 2010;135:481–494.

34. Gao YD, Garcia ML. Interaction of agitoxin2, charybdotoxin, and iberiotoxin with potassium channels: selectivity between voltage-gated and Maxi-K channels. *Proteins*. 2003;52:146–154.

35. Koehler RC, Gebremedhin D, Harder DR. Role of astrocytes in cerebrovascular regulation. *J Appl Physiol*. 2006;100:307–317.

36. Nystoriak MA, O'Connor KP, Sonkusare SK, Brayden JE, Nelson MT, Wellman GC. Fundamental increase in pressure-dependent constriction of brain parenchymal arterioles from subarachnoid hemorrhage model rats due to membrane depolarization. *Am J Physiol Heart Circ Physiol*. 2011; 300:H803–H812.

37. Knot HJ, Standen NB, Nelson MT. Ryanodine receptors regulate arterial diameter and wall $[Ca^{2+}]$ in cerebral arteries of rat via Ca^{2+}-dependent K^+ channels. *J Physiol*. 1998;508:211–221.

38. Jaggar JH, Li A, Parfenova H, Liu J, Umstot ES, Dopico AM, Leffler CW. Heme is a carbon monoxide receptor for large-conductance Ca^{2+}-activated K^+ channels. *Circ Res*. 2005;97:805–812.

39. Plueger S, Faulhaber J, Fuerstenau M, Loehn M, Waldschutz R, Gollasch M, Haller H, Luft FC, Ehmke H, Pongs O. Mice with disrupted BK channel beta1 subunit gene feature abnormal $Ca(^{2+})$ spark/STOC coupling and elevated blood pressure. *Circ Res*. 2000;87:E53–E60.

40. Sausbier M, Arntz C, Bucurenciu I, Zhao H, Zhou XB, Sausbier U, Feil S, Kamm S, Essin K, Sailer CA, Abdullah U, Krippeit-Drews P, Feil R, Hofmann F, Knaus HG, Kenyon C, Shipston MJ, Storm JF, Neuhuber W, Korth M, Schubert R, Gollasch M, Ruth P. Elevated blood pressure linked to primary hyperaldosteronism and impaired vasodilation in BK channel-deficient mice. *Circulation*. 2005;112:60–68.